Visualizing the geometry of the GBT metrology systems

Don Wells*

February 25, 1998

Abstract

This report presents an atlas of images of the GBT metrology systems rendered with NRAO's visualization workstation hardware using the "AVS" software system. These images illustrate geometric relationships between the metrology sensors and the structure of the GBT; they also illustrate methods for using visualization technology to study complicated geometry.

Contents

---

*mailto:dwells@nrao.edu

1   Introduction

In 1993, it became clear that there was a need for a flexible visualization capability to support planning for the GBT metrology systems. Around 1991 NRAO had purchased two IBM RS/6000 workstations with large memories (500 megabytes!), graphics accelerator hardware and the "AVS"[1] software system to support scientific visualization; these machines were installed in Charlottesville and in Socorro. The author investigated the possibility of using the Charlottesville system ringtail to visualize the GBT structural model [WK95], and found that a product called "UCD Builder"[2] could be used with AVS to read and display the structural model which had been computed by "MSC/NASTRAN"[3]. After some tests, the GBT project purchased the UCD Builder in the spring of 1994. By June 1994 we were able to insert arbitrary objects into the scene in order to visualize the metrology components (rangefinders, retroreflector prisms) in the context of the GBT structure. Later other objects (buildings, roads) were added to aid in visualizing the GBT in the context of its environment. Our implementation evolved steadily through 1994 and 1995 in the course of using it for a variety of geometric investigations for planning the metrology systems. In the spring of 1996 additional objects were added to represent the elevation axle, the azimuth wheels, the subreflector and certain roads in the neighborhood of the GBT. The representation of the details of the rangefinders was greatly improved and stick figures representing humans were added to aid visualization of the scale of the scenes. An important technology added in this stage of the development was the ability to render a rangefinder in arbitrary orientation using rotation matricies computed from Euler angles. In the winter of 1998, scenes were computed to visualize long paths through the air to a target on a nearby hillside and also to visualize measuring the orientation of the subreflector.

Figure 1[4] gives an overview of the GBT as seen in the AVS visualization system. We are looking northwestward toward the GBT; north is to the right. The GBT is pointed to the zenith, at azimuth 0° (North)[5]. The Comsat/RSi building is south of the telecope, and the roads around the telescope are shown. The "road" in the lower left corner of the scene is the old interferometer track, which is about 200 meters south of the GBT. The grid in the scene has 1000 inch (about 25 meter) spacing, and extends ±10000 inches from the origin of the XYZ coordinate system at the pintle bearing. The 12 ground-reference laser rangefinders are shown at 120 meters radius from the GBT. A human-shaped object is in the scene, standing near rangefinder ZY103 (cf. Figures 2 and 4), 120 meters east of the telescope. The rectangular object plotted near ZY103 and the human-shaped object represents the shield-room trailer which is currently being used to hold metrology computing equipment. The object northwest of the GBT is the new weather tower, which also appears in Figure 22 (p.26).

---

[1] Advanced Visual Systems, Inc., Waltham, MA; see http://www.avs.com/ and http://avs.ncsc.org/.

[2] Scientific Visualization Associates, Inc., Concord, MA, often referred to as "SciViz". This company is now out of business; the rights to some of their data conversion products were purchased by IBM for use with IBM's "Data Explorer" [DX] product, which is similar to AVS (see http://www-i.almaden.ibm.com/dx/). The "UCD" in the SciViz product name refers to the AVS data type "Unstructured Cell Data".

[3] The MacNeal-Schwendler Corporation

[4] atlas980219a.ps [25000,-8000,8000]↦[0,0,1000]23°[0,0,1]

Note: The notation used in this footnote gives the filename in directory /home/fits/dwells/avs_stuff/data/Pictures/atlas/, the XYZ location of the "camera" in inches, the XYZ location toward which the camera is pointed, the width of the scene in degrees and the unit vector which specifies the "up" orientation in the scene. The origin [0,0,0] is the pintle bearing at the center of the base of the GBT. For the purposes of these visualizations, $+X$ is taken to be East and $+Y$ is taken to be North (this is rotated 180° with respect to the definition of the alidade coordinate system given in [Kin94] and [KM93]). File atlas960503f.ps is actually a *color* Postscript file, and can be reproduced as a color print or viewgraph with the Tektronix "Phaser 560" printer in room 215 of the NRAO-Charlottesville Edgemont Road offices, or with the identical color laser printers located at NRAO-GB and other NRAO sites. A monochrome reproduction is somewhat harder to understand because of the color-coding information is missing. A compressed color Postscript file of this GBT memo is available at ftp://fits.cv.nrao.edu/pub/gbt_dwells_vis.ps.gz [2.3 MB compressed, 35 MB uncompressed].

[5] The GBT has this orientation in all scenes shown in this report.

Figure 1: Overview of the GBT visualization

Figure 2: Identification map for ground-based rangefinders

Figure 2[6] shows the proposed locations of rangefinders ZY101 through ZY112 superposed on the site plan of the GBT. The positions, sizes and orientations of the RSi building, the rangefinders and the roads as shown in Figure 1 were measured from this drawing.[7]

The early stages of this GBT visualization project were described in a poster paper [Wel94] presented at the ADASS-IV meeting.

---

[6]gbtzymap.ps

[7]This particular map is used in this figure because the labels such as 'ZY107' are large enough to reproduce well at this resolution. The current version of this map is revision 'B' (1996-10-21) of drawing D35420C004, which shows the drainage pond near ZY101 as it was actually built, to the left of ZY101 rather than to the right. Also, the whole ring of rangefinders was built at locations rotated slightly counterclockwise from those shown so that ZY104 would be farther from the road. In addition, D35420C004-B shows the weather tower northwest of the GBT.
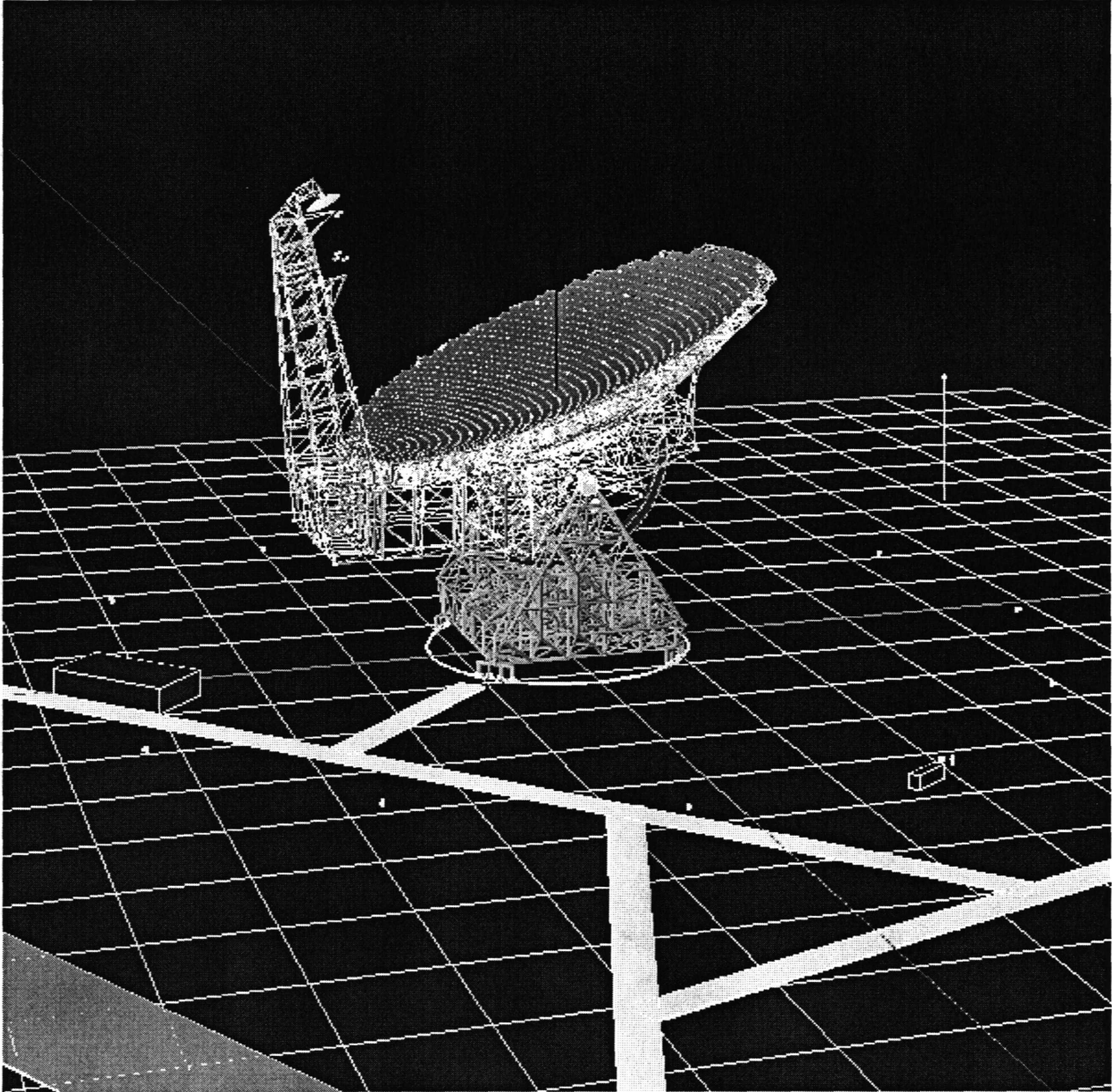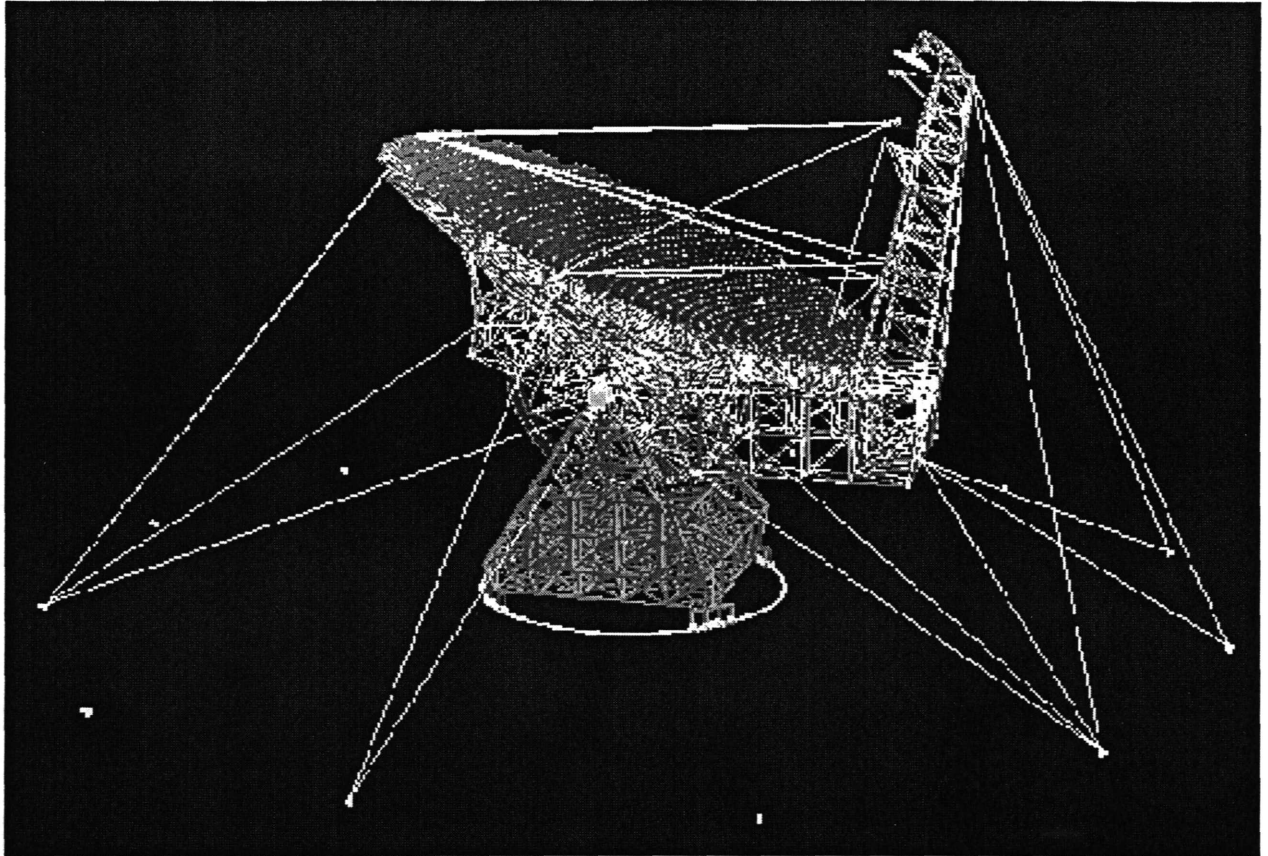
Figure 3: Overview of trilateration of alidade, tipping structure and surface

2 Trilateration of the structure & surfaces (Lines-of-sight)

During the process of implementing arbitrary orientations of rectangular solids and cylinders in order to visualize the rangefinders, code was added to draw "lines" between arbitrary pairs of points. These lines are modelled as cylinders, generally with diameter one inch. In Figure 3[8] such lines are drawn connecting various groundbased rangefinders to retroreflectors on the elevation bearing, the box under the backup structure, the edge of the parabolic dish and the tip of the feedarm. Lines are also drawn connecting rangefinders on the feedarm to retroreflectors on the surface of the parabolic dish. Lines of sight to the edge of the dish from both ground and feedarm enable the coordinates of arbitrary points on the surface of the dish to be tied to fixed points on the ground.

2.1 The "ring of fire" — measuring the orientation of the tipping structure

Figure 4[9] shows a view of rangefinder ZY103, with the GBT in the background and the nearby stick figure on the left side of the scene. The rangefinder's steering mirror is 60 inches above the ground, and the base of the instrument is pointed toward the GBT. The housing of the instrument blocks lines of sight from the steering mirror to points on the lower part of the alidade, but the three lines shown in the figure demonstrate that the retroreflector under the elevation bearing is visible,[10] as is the edge of the dish and the adjacent

---

[8] atlas980217a.ps [-15000,-4300,5000]↦[0,0,1000]40°[0,0,1] This figure also appears in [HGPP98].

[9] atlas980219b.ps [4320,2065,60]↦[0,-4000,1700]80°[0,0,1]

[10] Actually, the alidade elevator, which is not modelled here, probably blocks this particular line.
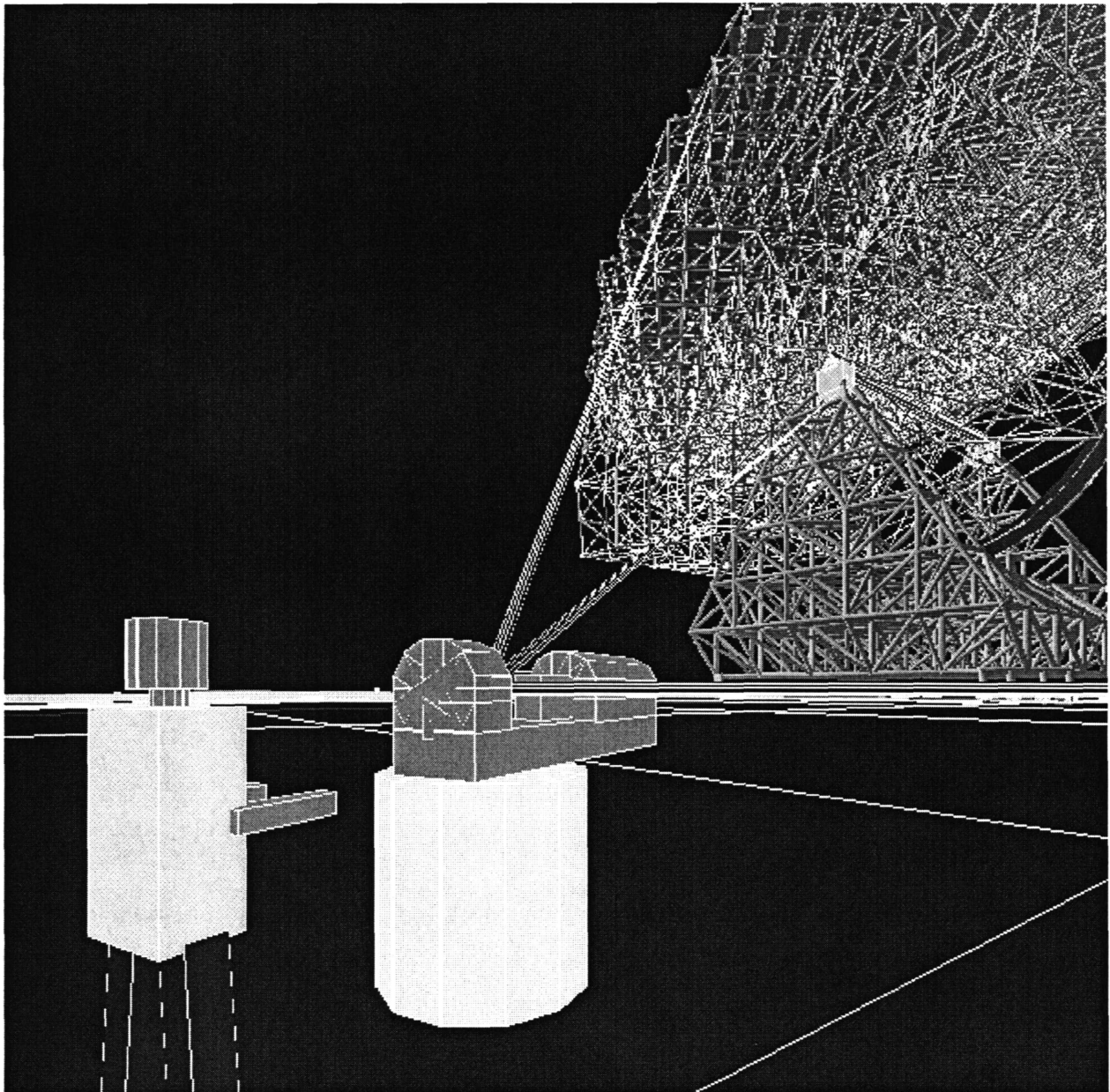
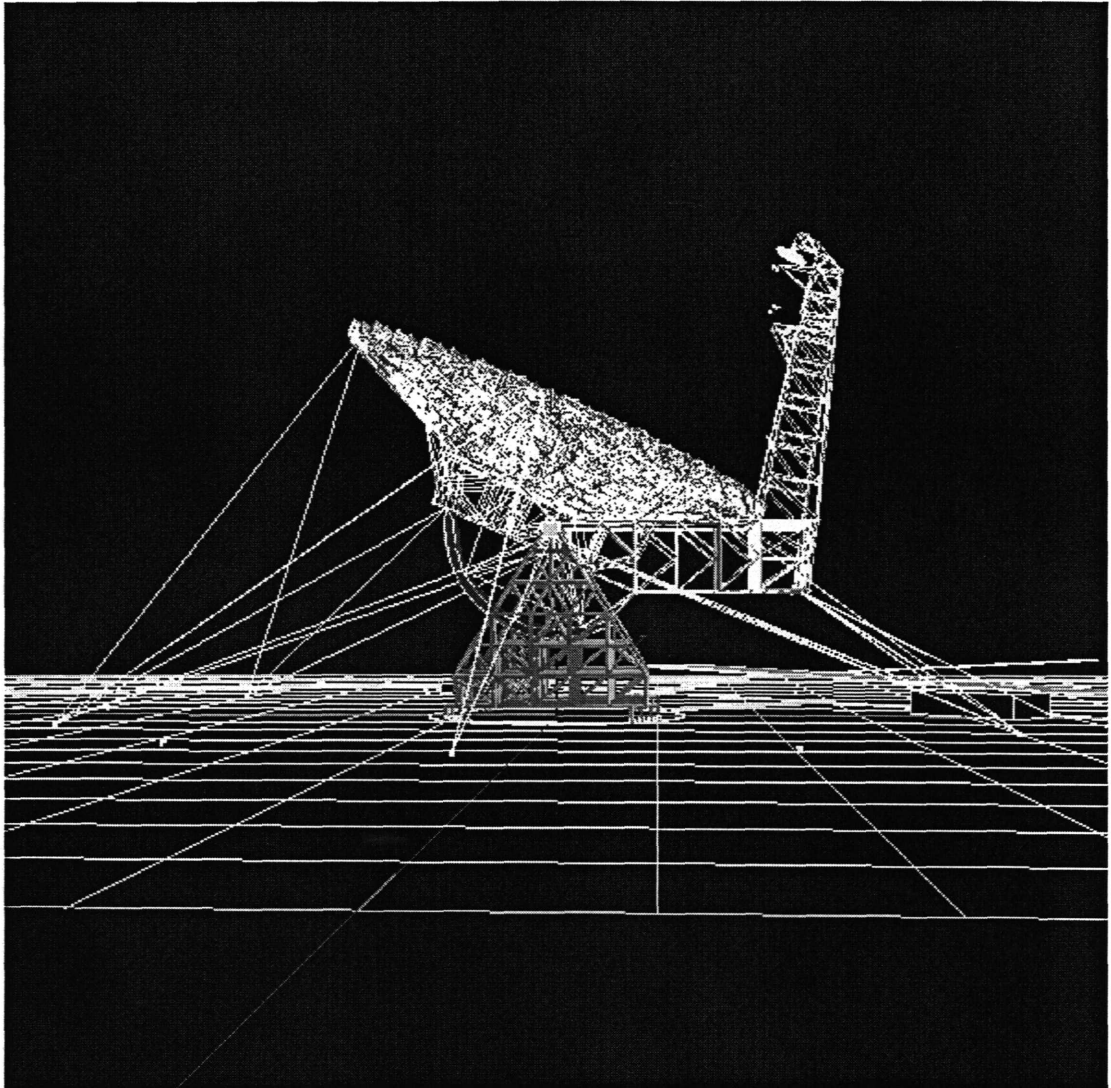Figure 4: Lines-of-sight from Ground-based rangefinder ZY103 to the GBT & ZY101

Figure 5: Determining the orientation of the tipping structure

rangefinder ZY101.

In Figures 5[11] and 6[12] we see two views of various lines of sight from groundbased rangefinders to retroreflectors on the tipping structure. The reader can examine Figure 5 and imagine the structure tipping counterclockwise to elevations other than 90°; It is clear that the relative importance of various rangefinders in measuring the elevation of the structure will change, but that favorable angles are still available. The groundbased rangefinders can measure the position of each elevation bearing in all three coordinates; the reader can compare these figures with Figure 4 of [Gol97]. Only a fraction of the possible lines are shown— there will be *twelve* groundbased rangefinders, so there will be plenty of redundancy in the measurement system!

---

[11] atlas980220a.ps [-15000,-1000,1000]↦[0,0,1700]40°[0,0,1]
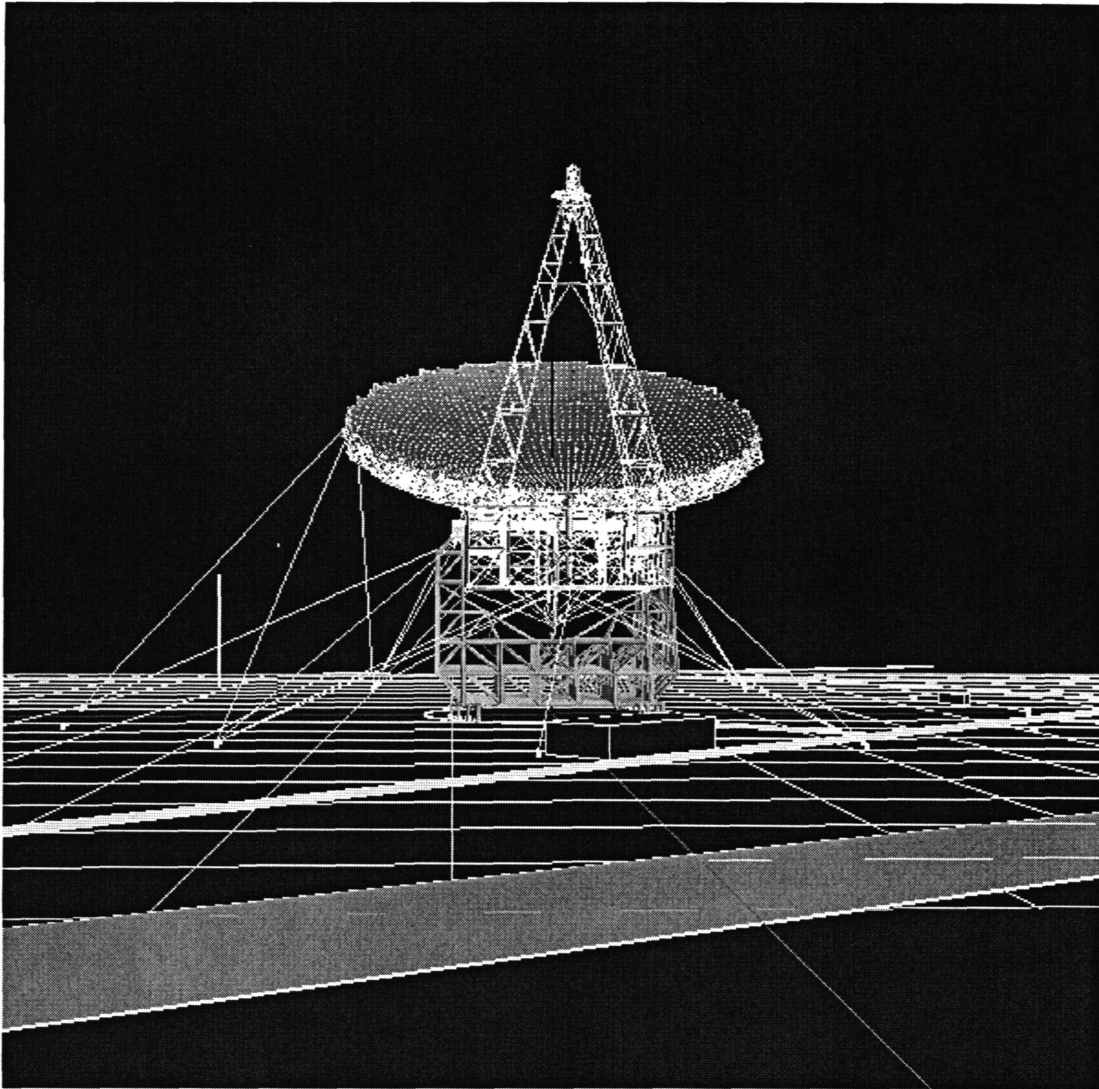[12] atlas980220b.ps [-1000,-15000,1000]↦[0,0,1700]40°[0,0,1]

Figure 6: Determining the orientation of the tipping structure

2.2   The six rangefinders on the feedarm

Six laser rangefinders will be installed on the GBT feedarm, four around the Gregorian feedroom and two on the legs of the feedarm. The rangefinders have a limited solid angle coverage, but the targets for the different applications of these metrology devices are scattered over a rather large solid angle. The AVS system was used repeatedly in 1994-1996 to refine our ideas about how the competing requirements can best be met with the technology. Mainly, the AVS system has been used to choose the best *locations* for the six rangefinders. It is also important to optimize the *orientation* of the devices, to match the solid angle coverage to the targets. This optimization has been done with Mathematica algorithms developed by Schwab[Sch96], who has recommended optimum orientations for the six rangefinders. Schwab's report tabulates Euler angles and equivalent rotation matricies for the orientations, and shows plots of the solid angle coverage and targets. It is, however, somewhat difficult to imagine the orientations of the instruments when looking at the solid angle plots in [Sch96]! During April-July 1996 the AVS visualization code was enhanced so that it could plot models of the rangefinders oriented by arbitrary Euler angles in order to aid the interpretation and implementation of Schwab's results.

2.2.1   The four rangefinders around the feedroom

Figure 7[13] shows the four rangefinders located around the Gregorian feedroom. The devices are on their sides so that both the main reflector and the subreflector can be reached by the roll angles available to the steering mirrors. The optical axes of the instruments are not parallel to the roof of the feedroom, but rather are angled outward. The two stick figures in the scene are 68-inches high. Note the two cardinal points at the rear top of the feedroom, as specified in [Kin96a].

These instruments have different *names* in different memos; the correspondence table given below is based on Figure 2 of [Sch96], the P_i' table of coordinates on page 4 of [Sch96] and the P4=ZY113 table in [Par96]:

Name in [Par96]	Id in [Sch96]	X (in)	Y (in)	Z (in)	ϕ (deg)	θ (deg)	ψ (deg)	Description
ZY113	P4	+482.48	-2141.22	2807.95	42.36	124.16	10.31	lower part
ZY114	P3	-482.48	-2141.22	2807.95	137.64	124.16	169.69	of feedarm
ZY115	P6	+305.28	-2344.74	3786.17	26.91	112.68	16.51	bottom rear
ZY116	P5	-305.28	-2344.74	3786.17	153.09	112.68	163.49	of feedroom
ZY117	P2	+151.50	-2149.87	4039.22	19.63	110.60	8.74	top front
ZY118	P1	-151.50	-2149.87	4039.22	160.37	110.60	171.26	of feedroom

The six rangefinders are rendered at these XYZ positions and with these Euler angles[14] in the images shown here. In Figure 7 the names of the rangefinders from left to right are ZY115 (P6, at bottom rear of feedroom), ZY117 (P2, at top front of feedroom), ZY118 (P1) and ZY116 (P5), respectively. $+X$ is to the left.

Figure 8[15] is a closeup view of rangefinder ZY118 (P1) on the roof of the Gregorian feedroom. We see that it is turned on its side. The two housings at the ends of the instrument are rounded; these housings limit the solid angle coverage of the steering mirror. The small rectangular unit between the two rounded end units represents the optics device housing. The steering mirror (the fiducial point of the rangefinder) is rendered in a contrasting color.
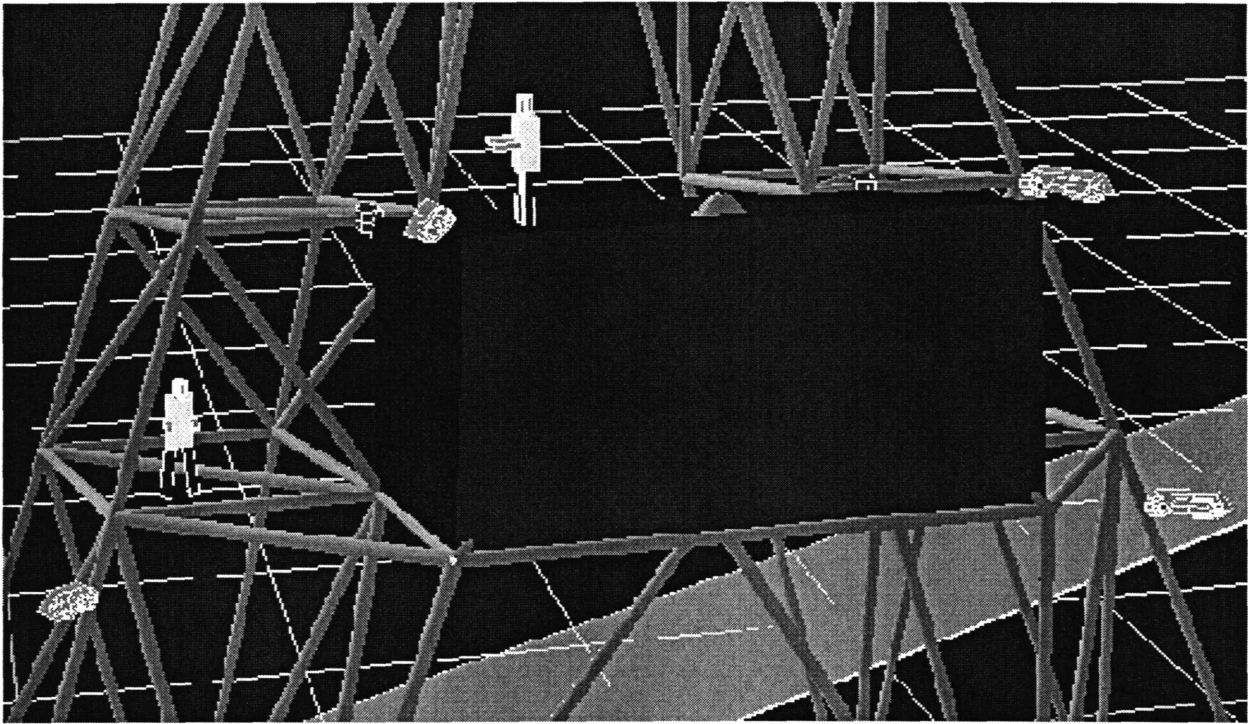
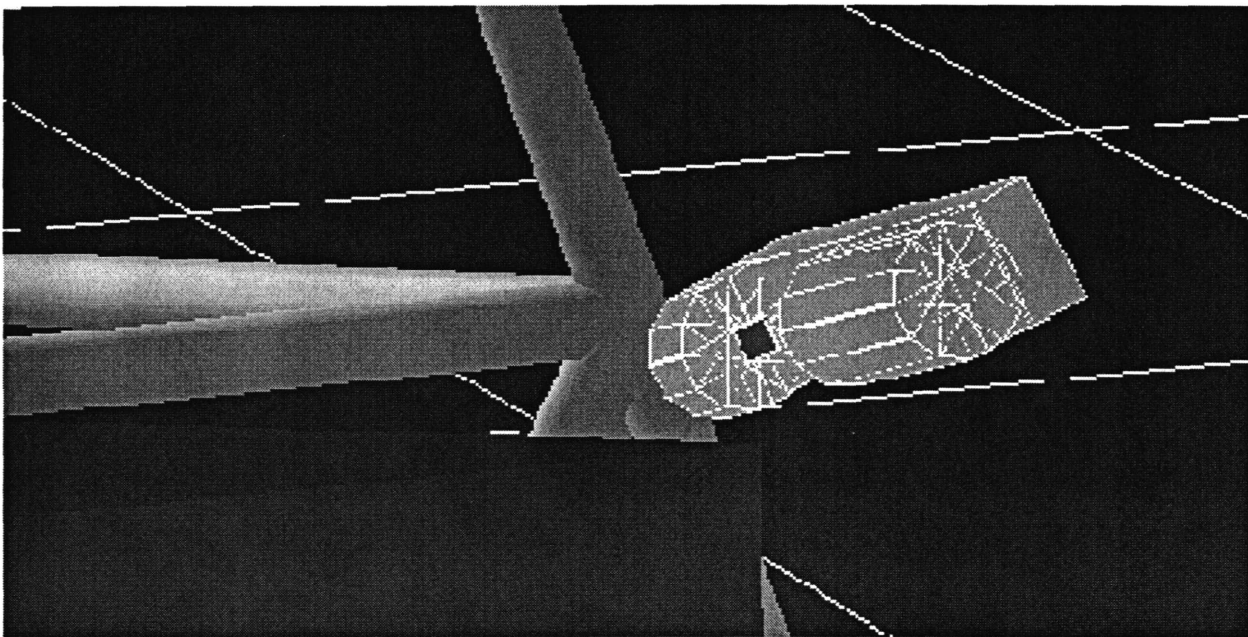Figure 7: Rangefinders ZY115, ZY117, ZY118 and ZY116 around the Gregorian feedroom

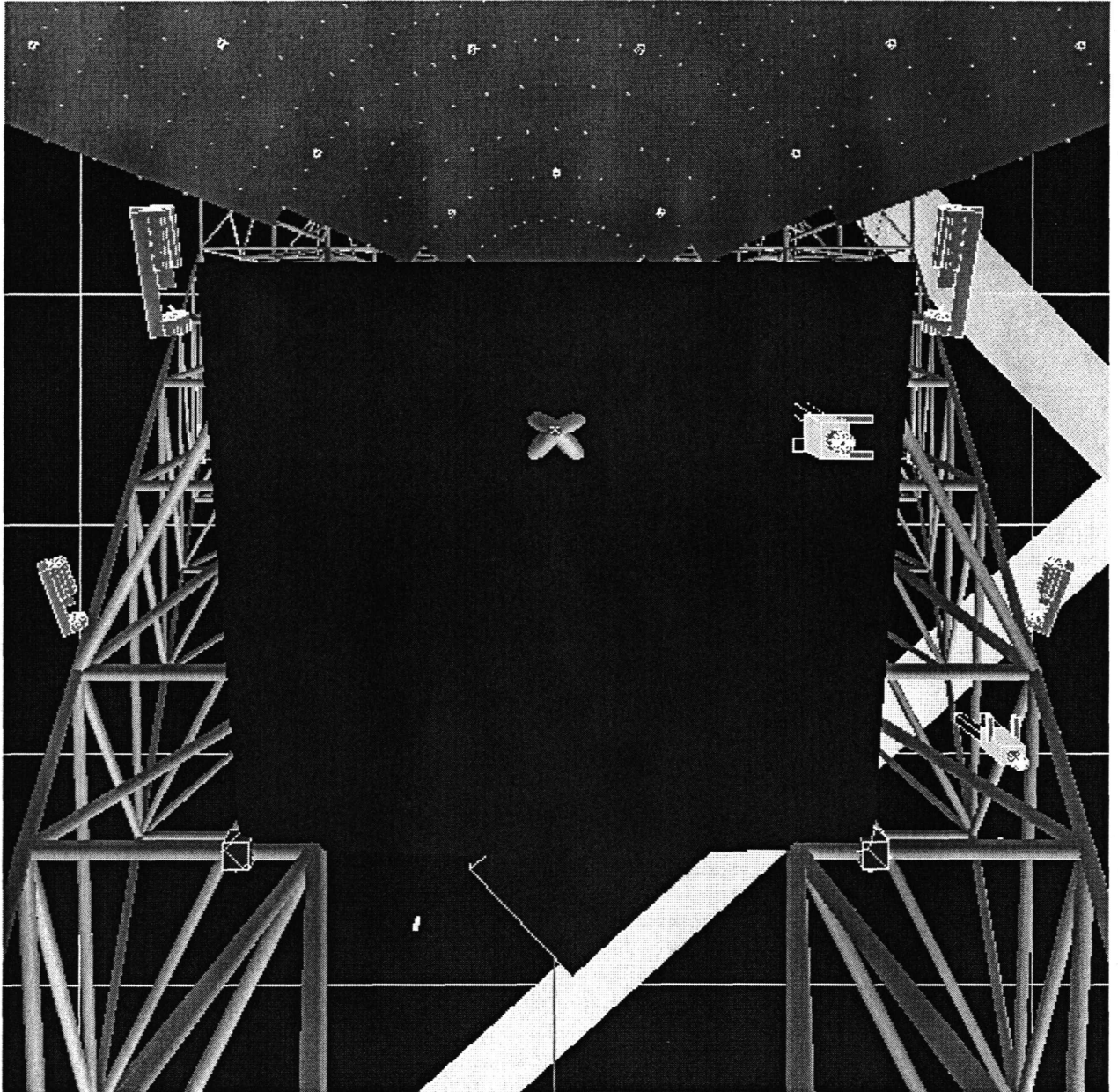Figure 8: Closeup view of rangefinder ZY118 (P1) on the roof of the Gregorian feedroom

Figure 9: Looking down from the prime focus toward the feedroom roof

2.2.2   The view from the top

Figure 9[16] is looking down from the prime focus feedhorn toward the Gregorian focus feedhorn, with $+Y$ vertical in the scene. Again we see that the rangefinders are on their sides and angled outward slightly, and this time we see the stick figures from above. There are three problems with Figure 9:

- The top front edge of the feedroom overlaps the edge of the beam converging from the main mirror (the camera is at the prime focal point), *but this is incorrect!* When we first saw this overlap in the visualization system in 1994, a check of the final design of the feedroom was made, and it was determined that the front edge of the feedroom will comfortably clear the converging wavefront. The front edge is not in the final location in the NASTRAN model; a line connecting the steering mirrors of ZY117/118 will be in front of the edge.

- The housings of rangefinders ZY117/118 are shown very close ($\approx$ 20 cm?) to the edge of the converging beam, *probably closer than in the final design.* This is because the rangefinders are shown in these visualizations with their covers opened but not removed. The baseplates of the instruments are only about 36 inches long, not the 51.4 inch length shown here. Also, the clearance between the beam and the instruments can be increased by moving the rangefinders outward.

- A portion of the RSi building is shown beneath the Gregorian feedroom, *but this is incorrect!* There will be one floor at the level of the feedroom and another floor at the level of the prime focus boom in its retracted position, and both of these floors (which are not included in our model) will block this line of sight.[17]

The objects at the lower left corner and lower right corner of the feedroom roof mark two of the structural cardinal points specified by King[Kin96a]; presumably retroreflector prisms will be installed at these points for measurement by the ground-based rangefinders.

It is desirable that the two rangefinders ZY117 and ZY118 at the top front edge of the feedroom should be able to range on each other and also be able to range on the Gregorian feed if at all possible; the latter possibility will facilitate measurement of the X-Y coordinates of the Gregorian feedhorn in the same coordinate system in which the rangefinders will be measuring the main mirror and the subreflector positions.

2.2.3   The view from the side

The upper part of the GBT feedarm is shown from the side in Figure 16 (p.20). The 68-inch stick figures standing on the subreflector backup structure, the platform adjacent to the feedroom and on the feedroom roof give a sense of the scale of the feedarm. We see the structural cardinal points on the prime focus boom. From this angle we can see that the two rangefinders ZY115 and ZY116 at the bottom rear of the feedrom can range on each other on a line-of-sight passing beneath the feedroom (*cf* Figure 9 of [Sch96]).

---

[13] atlas960503c_crop.ps [400,-800,4400]↦[50,-2245,3900]25°[0,0,1]

[14] In the implementation used here, the rangefinder is rotated by $-90°$ about Z to get to the same canonical orientation as in [Sch96], then by $\phi' = \phi - 90°$ about Z, by $\theta' = -\theta$ about X and by $\psi' = \psi + 90°$ about Z; the three primed rotations account for the fact that the axis convention used here is different from that used in [Sch96].

[15] atlas960618a_crop.ps [400,-800,4400]↦[-151.5,-2150,4039]5°[0,0,1]

[16] atlas960618b.ps [0,-2159,4459]↦[0,-2250,4028]55°[0,1,0] (note that $+Y$ is vertical)

[17] The small object shown to the left of the building is rangefinder ZY107 seen from above (cf. Figure 2). If the line of sight were clear, the fact that ZY107 is visible in this scene would imply that it could range on the two cardinal points on the prime focus feedbox in this orientation of the GBT ($A = 0, E = 90$). This is an illustration of a typical tactic which can be used in these geometrical studies: put the camera at a target location and look around to see which rangefinders are visible. For example, the fact that the steering mirrors of the four rangefinders around the feedroom are visible implies that all of them can range on the PF box, which should enable measurement of the location of the feedbox in the same coordinate system in which these rangefinders will measure the surface of the primary mirror.

2.2.4   The two rangefinders on the lower part of the feedarm

Rangefinders ZY113 (P4) and ZY114 (P3) are to be located on front face of the feedarm(s), at the second truss joint above the main dish. The four rangefinders around the feedroom will work together with these two lower rangefinders to trilaterate on the main dish and the subreflector, and the angles involved are easy to visualize in Figure 11 (p.15). In Figure 14 (p.17) we zoom in to display the orientations of the two lower rangefinders as specified in [Sch96].

2.3   Measuring the active surface

Figure 10[18] shows the main reflector as seen looking straight down from a height of 2500 feet. The locations of the 2209 actuators (retroreflector prisms) at the corners of the panels can be seen as faint white dots. The dots which are highlighted are the 94 nodes which have been designated as "cardinal points" by Lee King in [Kin96b] (see Figure 12[19]). Lines of sight are shown from ZY118, ZY113 and ZY114 to nodes -742030, 748009, 700001 and 700045 to illustrate the angles involved in triangulating to various points on the surface. Figure 11[20] shows the same lines viewed from the side, from the same distance, with the same FOV as figure 10.

Figures 10 and 11 suggest that solutions for Y-coordinates of nodes near the vertex and Z-coordinates near the outer edge will have the largest error bars. The wavefront error does not depend on Y near the vertex, and for large radii the geometry for measuring displacements normal to the surface (the important case) is more favorable than for measuring Z.

Figure 13[21] is what one of the cardinal point retroreflectors on the surface[22] can "see" with its $\pm 25°$ field of view. In this case, well away from the plane of symmetry and close to the feedarm (essentially the worst situation), all six of the rangefinders on the feedarm are visible, and therefore can measure ranges to this retroreflector, but several of them are nearly at the visibility limits.[23] If the rangefinders were moved to the outer edges of the feedarm, rather than the middle location that was chosen, the gain loss might be unacceptable.

Figure 14[24] is a closeup view of ZY113 and ZY114 which shows the lines-of-sight to the surface panels and to ZY118. We see that the various rays, which span most of the solid angle of interest, do not intersect the housing of the rangefinders.[25]

---

[18] atlas960701a.ps [0,-200,30000]↦[0,-200,2600]9.5°[0,1,0]

[19] mod95b.ps.feb2296; rotated 180° with respect to Figure 10, and only shows half of the symmetric pattern.

[20] atlas960701b.ps, [30000,-200,3500]↦[0,-200,3500]9.5°[0,0,1]

[21] atlas960624a_crop.ps, [720,-1520,2187]↦[0,-2123,3100]50°[0,1,0]

[22] The coordinates of node 748009, and of the other surface nodes, were taken from the convenient table of coordinates of GBT structural model nodes (joints) smTippingModelNodeTable.ps (330 KB, 21 pages landscape), which is included in the compressed file ftp://fits.cv.nrao.edu/pub/gbt_dwells_doc.tar.gz (538 KB); see [WK95] for background information on this table.

[23] Note that the line-of-sight from 748009 to ZY116 might be blocked by the support beam underneath the feedroom and that the LOS from ZY113 to ZY118 may be blocked by the horizontal beam at the bottom front edge of the feedroom (this needs to be checked!) The LOS from 748009 to ZY118 will *not* be blocked, as discussed in 2.2.2 (p.12).

[24] atlas960702a_crop.ps, [10000,-1850,2700]↦[-482,-2141,2820]0.5°[0,0,1]

[25] The dimensions of the rangefinder were taken from drawing D35420M145 (1995-08-10).
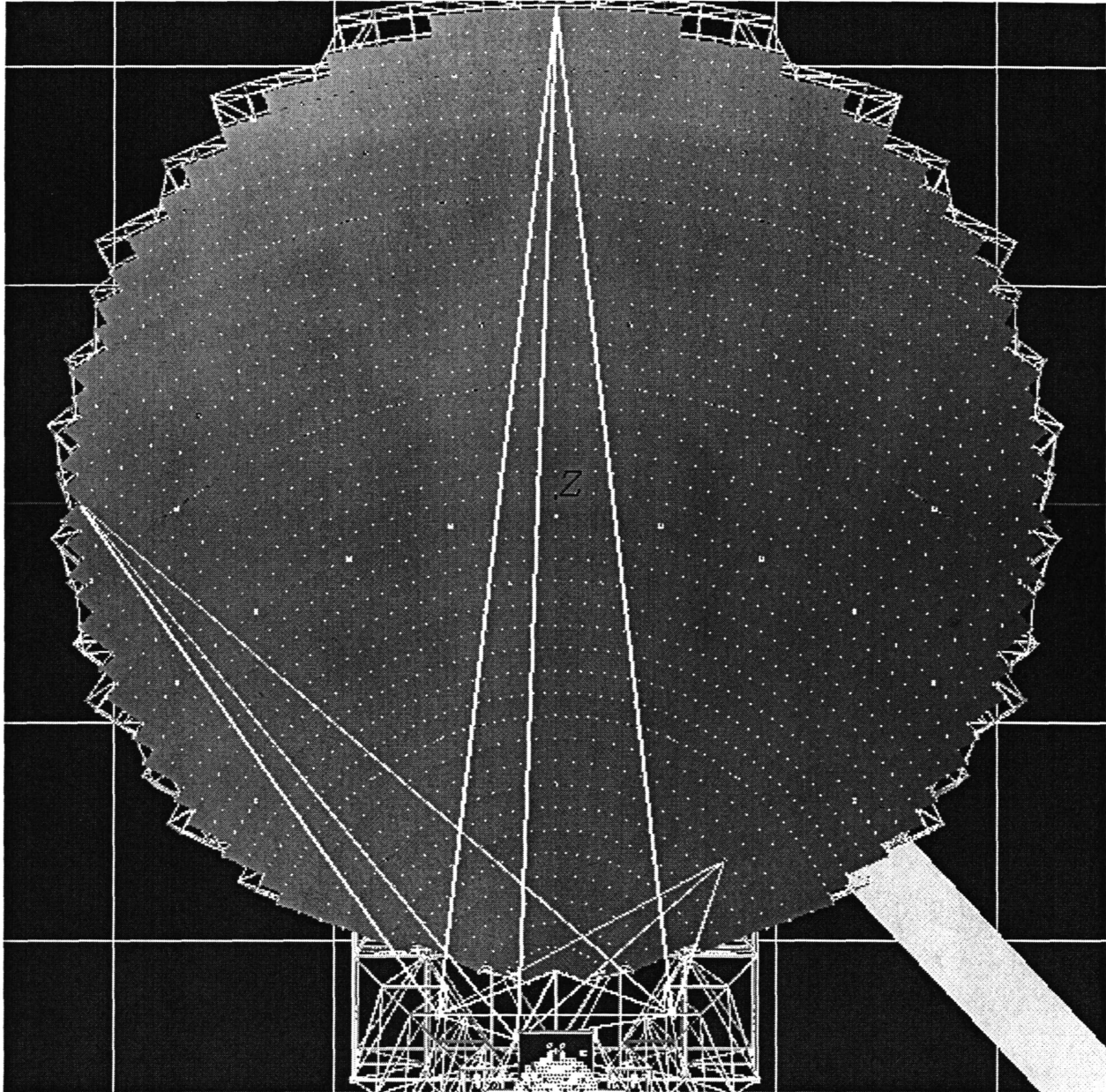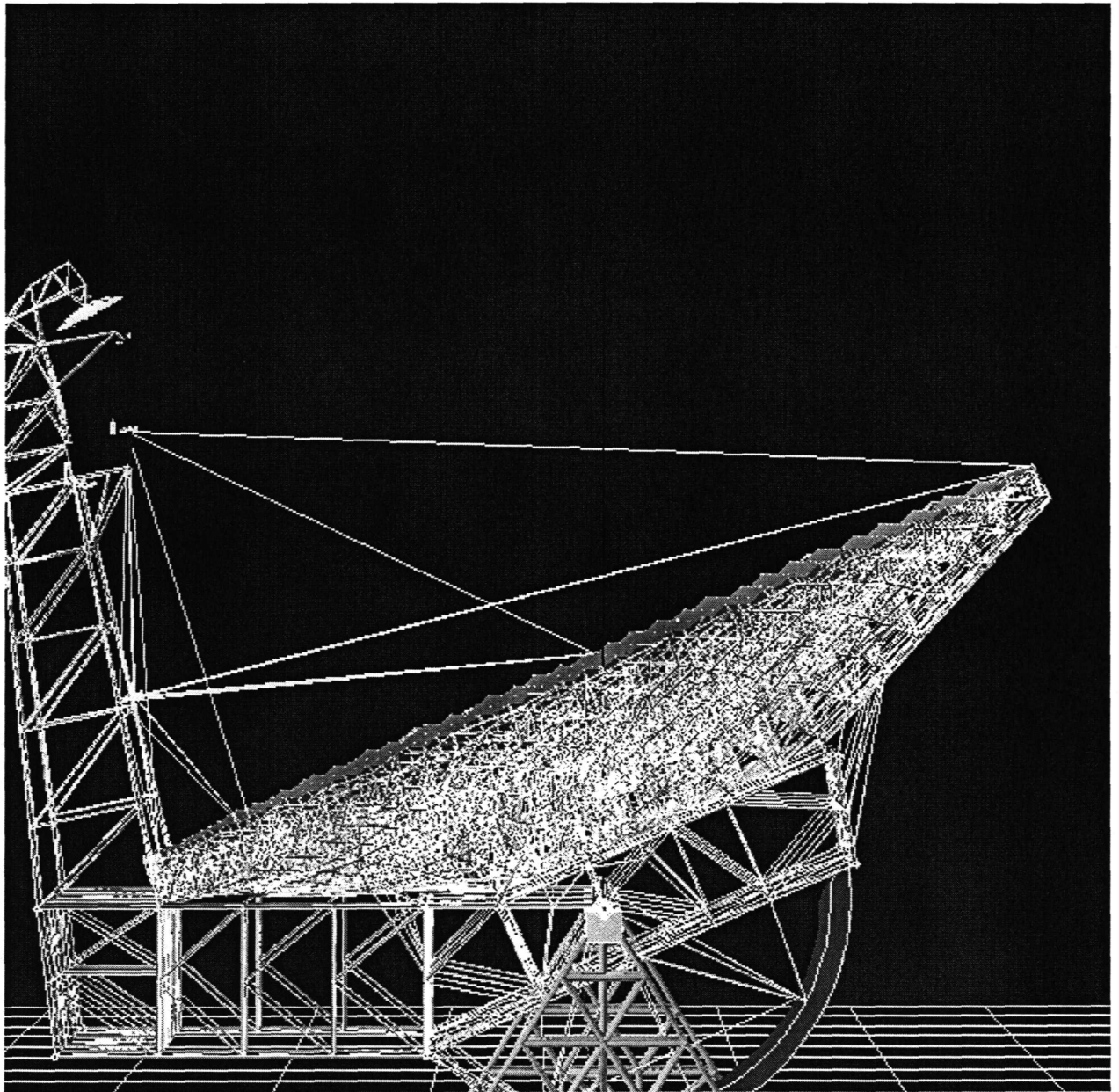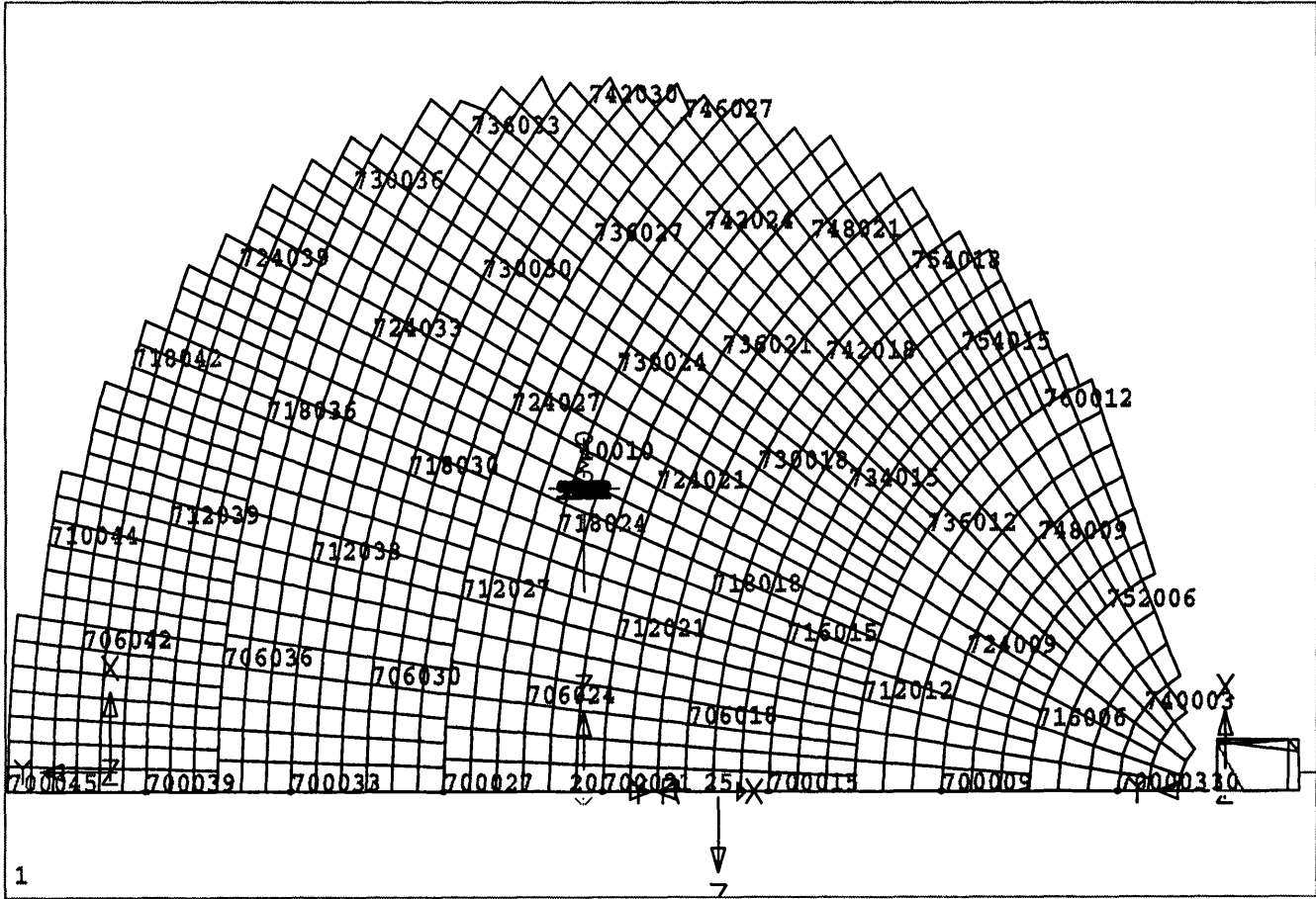
Figure 10: Surface servo geometry from above

Figure 11: Surface servo geometry from the side

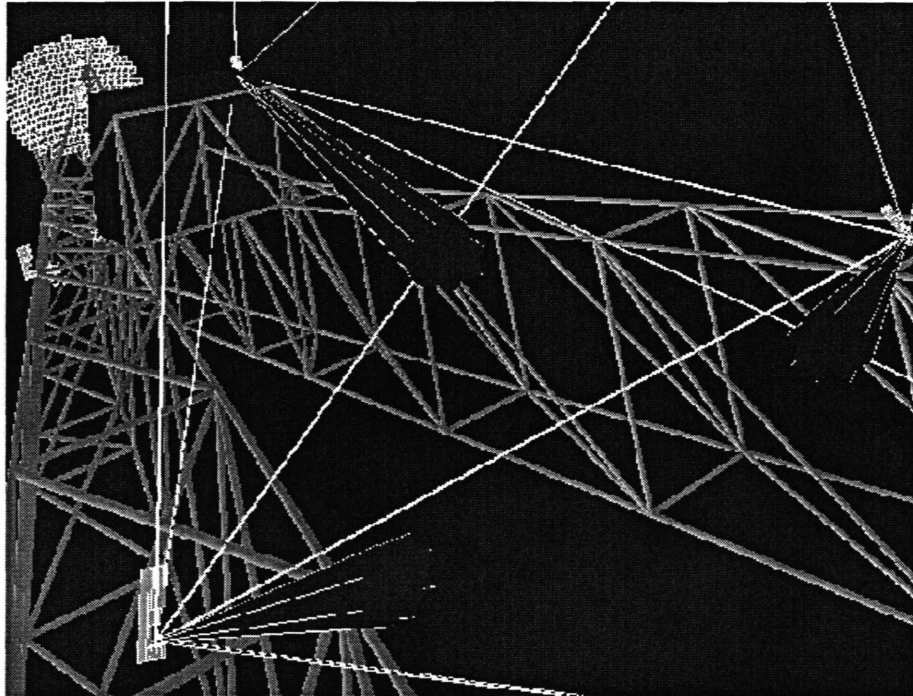Figure 12: Cardinal point node-ID identification map from [Kin96b]

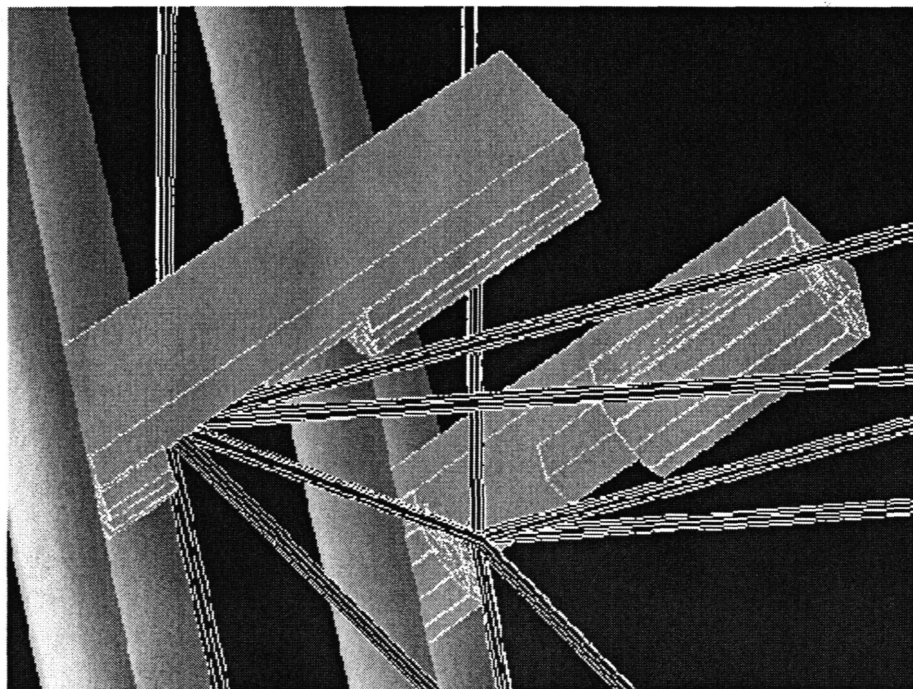Figure 13: The feedarm rangefinders as seen from cardinal point node 748009 with ±25° FOV

Figure 14: Lines-of-sight from ZY113 & ZY114 to surface retroreflectors and ZY118

2.4 Measuring the Subreflector

Figure 15[26] shows lines-of-sight from three of the four rangefinders around the feedroom to three of the six retroreflectors on the subreflector. It is clear that the angles of the lines for determination of the Z_s and Y_s coordinates and the X_n tilt of the subreflector by trilateration are reasonably favorable. Figure 16[27] shows the same lines as seen from the side, and the angles of the lines are favorable for determination of the X_s position and the Z_s tilt. The two figures make it obvious that the four rangefinders can also determine the position of the prime focus boom.

There are three human-shaped objects in these scenes: one standing on the back (top) of the subreflector, one standing on top of the feedroom and one standing near ZY115. These figures also appear in Figures 7 (p.10) and 9 (p.11). The peculiar texture of the subreflector in these scenes is due to the crude modelling of its surface as a set of flat plates 16 inches square, in horizontal orientation and placed at a set of points in the surface of the ellipsoid. The flat plates are seen more clearly in Figure 19 (p.24).

The coordinates of the surface points and of the six retroreflectors were supplied by Fred Schwab.

---

[26] atlas980216a_crop [0,10080,5000]↦[0,-2420,4280]5°[0,0,1]

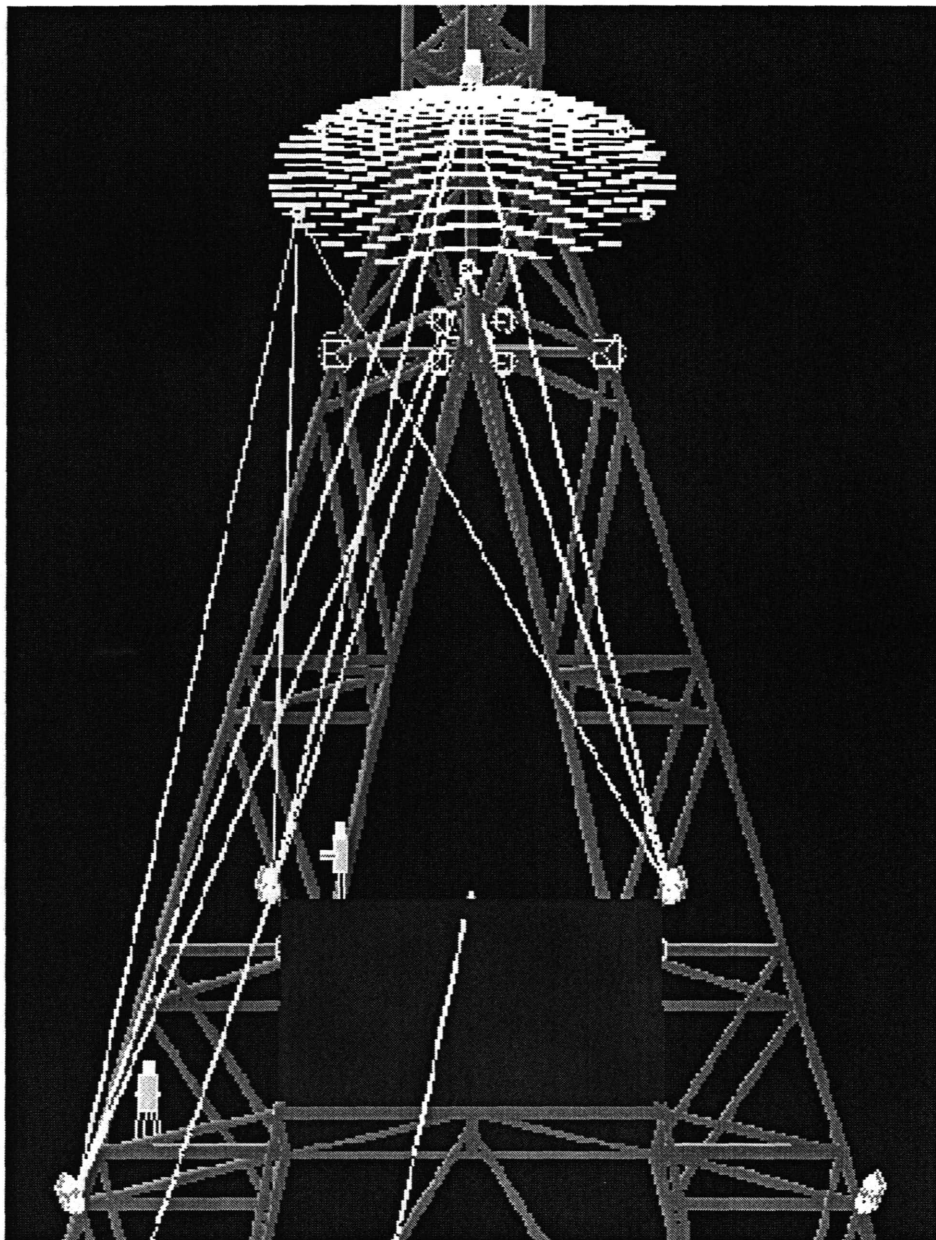[27] atlas980216b_crop [12500,-2500,5000]↦[0,-2420,4280]5°[0,0,1]

Figure 15: Lines-of-sight to the six subreflector retroreflectors (front view)
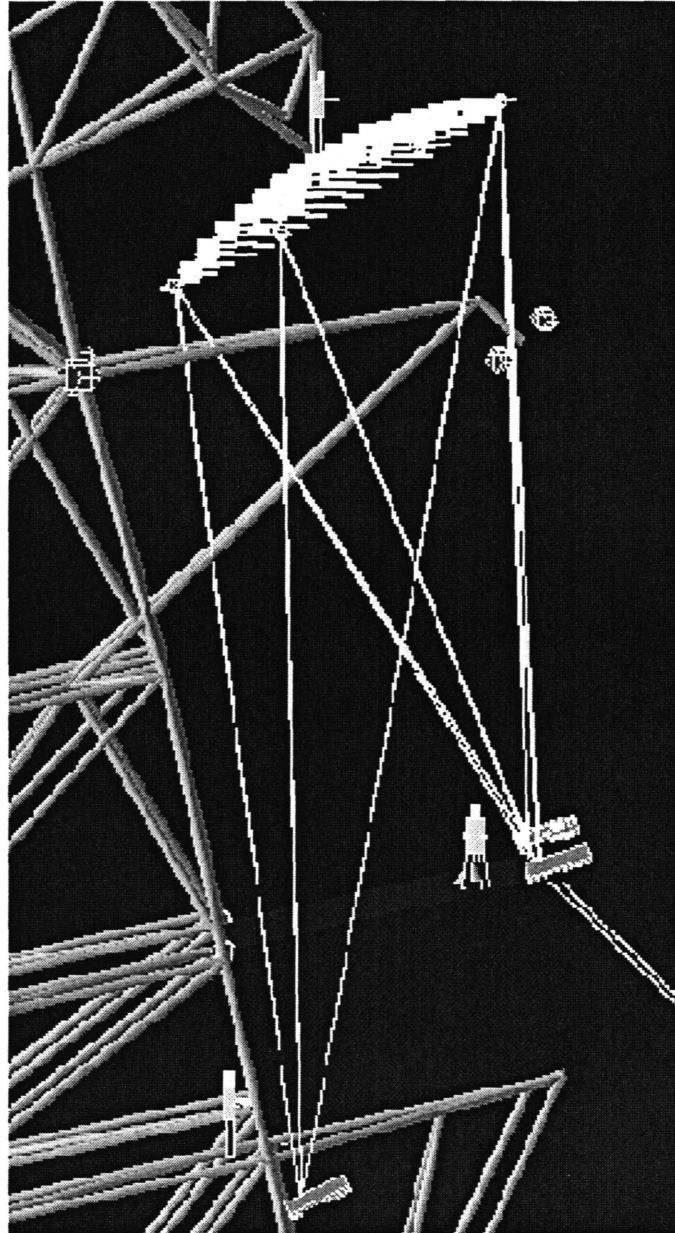
Figure 16: Lines-of-sight to the six subreflector retroreflectors (side view)

3   The quadrant detector

The quadrant detector consists of a transmitter which sends a collimated beam and a receiver unit which measures the X-Y intersection point of the beam at another location [PS96]. The transmitter is rigidly attached to the truss structure and does not steer the beam in any way, but the position of the transmitter and the direction of its beam will vary as a function of elevation as the truss structure distorts due to gravity. Distortions due to vibrations and other disturbances will also occur; a major goal for the quadrant detector is to monitor the feedarm motions of the first and second vibrational modes of the GBT. The receiver unit is also rigidly attached to the truss structure, but its position will also vary (receiver tilt perturbations will have negligible effect). The receiver produces two signals proportional to the X-Y position of the point where the transmitted beam intersects the plane of the receiver. The two signals depend on the position and tilt of the transmitter and on the position of the receiver. Range is not measured by the quadrant detector, but we could add a rangefinder sensor operating over a parallel path. The goal is to measure motions of the tip of the feedarm relative to the lower part of the tipping structure, either the backup structure of the main dish or the elevation axle. The vertex of the paraboloid is one plausible location. The other possibility is to mount the transmitter on a node near the elevation axle, as was discussed in [Nor96]. Two different locations for the receiver unit have been considered: the front edge of the feedroom and above the feedroom on the feedarm itself. The final decision had not been made by the date of this memo, and so the scenes shown here illustrate one plausible combination.

In Figure 17[28], the group of four highlighted nodes just to the right of the center of the dish are the corners of a particular panel which was identified as intersecting the line-of-sight for one proposed location — node 10230[29] — for the quadrant detector transmitter, as discussed in [Nor96] (cf figures 10 and 12 of that memo and also figure 2 of [Pay95]). Node 10230 has special significance: it is the upper termination point of the elevation encoder backshaft.[30]

In Figure 18[31], we see the line of sight originating at node 10230, which is marked as a cardinal point, and passing through the panel with the marked corners. The horizontal object in the lower part of the scene represents the elevation axle. The arrangement of the truss members makes it obvious that node 10230 is well-coupled to the axle, to the box structure and therefore to the backup structure of the parabolic dish.

Figure 19[32] illustrates how the quadrant detector beam can clear the feedroom roof on the path from node 10230 to the suggested location for the receiver, just above the prime focus boom and just below the subreflector. Readers should be aware that there are large deflections of the feedarm as elevation changes, which implies that the intersection point and feedroom clearance of the quadrant detector line-of-sight will change with elevation. In particular, the clearance between this line-of-sight and the L-band Gregorian feedhorn should be checked.

The two signals produced by the quadrant detector in this configuration can be modelled by obtaining the translation and tilt of node 10230 and the translations of nodes ±41040 (the two cardinal points on either side of the receiver in Figure 19) from the structural model [WK95], and combining them in a calculation similar to the "Displacement of Second Focal Point Relative to Feedhorn" situation described in Section 3.2 and Table 2 of [WK95]; section 2.0 of [Nor96] describes program qd which makes this calculation.

---

[28] atlas980220d, [-30,-2530,4500]↦[0,-600,2500]80°[0,0.707,0.707]

[29] Each node of the structural model has been given a unique integer ID code. The actual values of the integer codes have no particular significance, except that the leading digits generally indicate particular sub-structures of the structure. The "grid coordinates" for the node IDs are tabulated in a convenient form in the Postscript document smTippingModelNodeTable.ps (330 KB) which is included in the compressed tar file ftp://fits.cv.nrao.edu/pub/gbt_dwells_doc.tar.gz (516 KB).

[30] The GBT elevation encoder is not attached to the main elevation axle, rather it is attached to a 'backshaft', a T-shaped tube which terminates at the bottom and top (at node 10230) of the box structure, and is independent of the axle main structure (see Figure 3 of [Nor96]).

[31] atlas980220e, [620,400,1840]↦[463,-78,2074]50°[0,0,1]

[32] atlas980220c.ps [2000,7500,3500]↦[20,-2400,4434]20°[0,0,1]
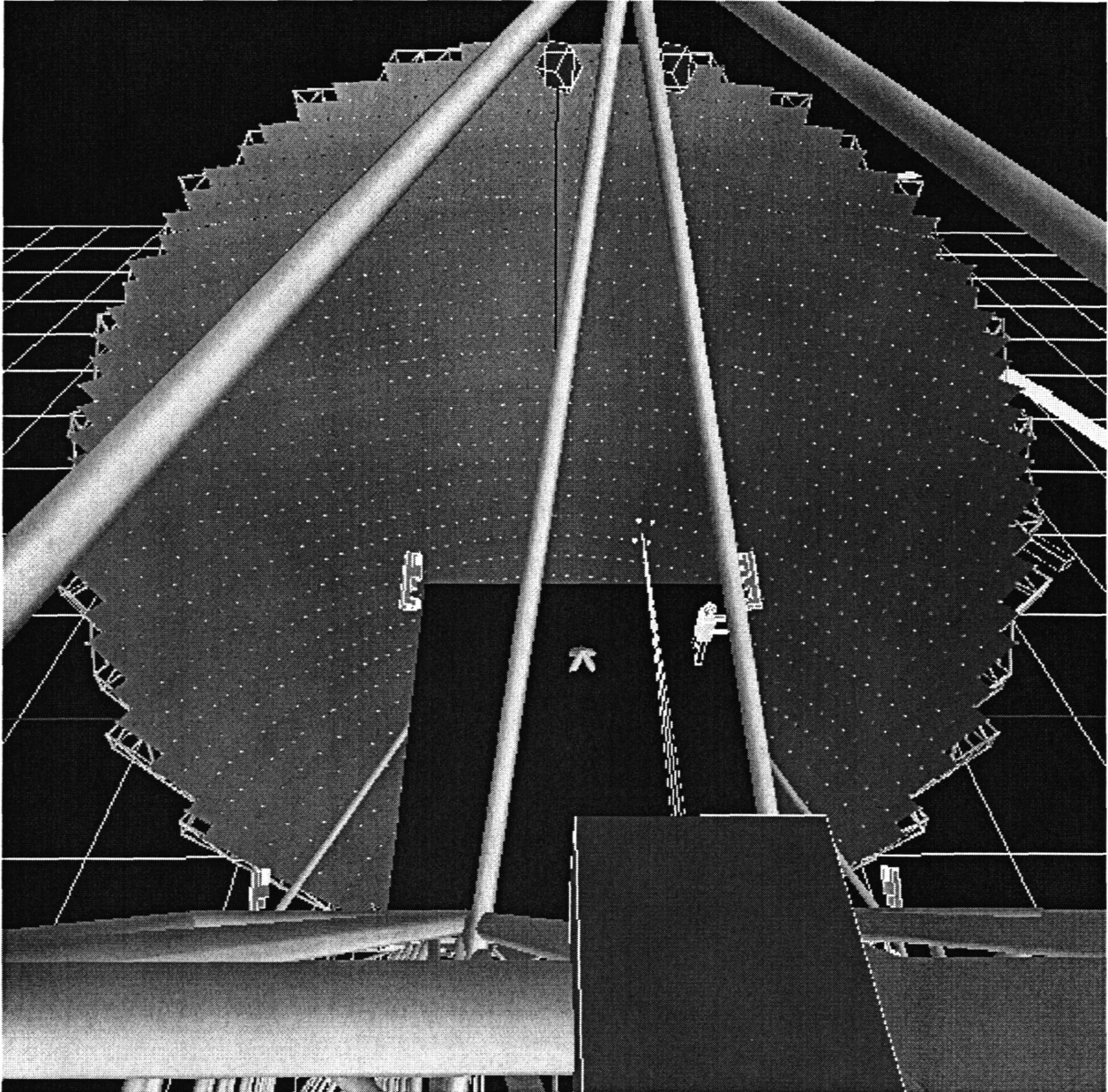
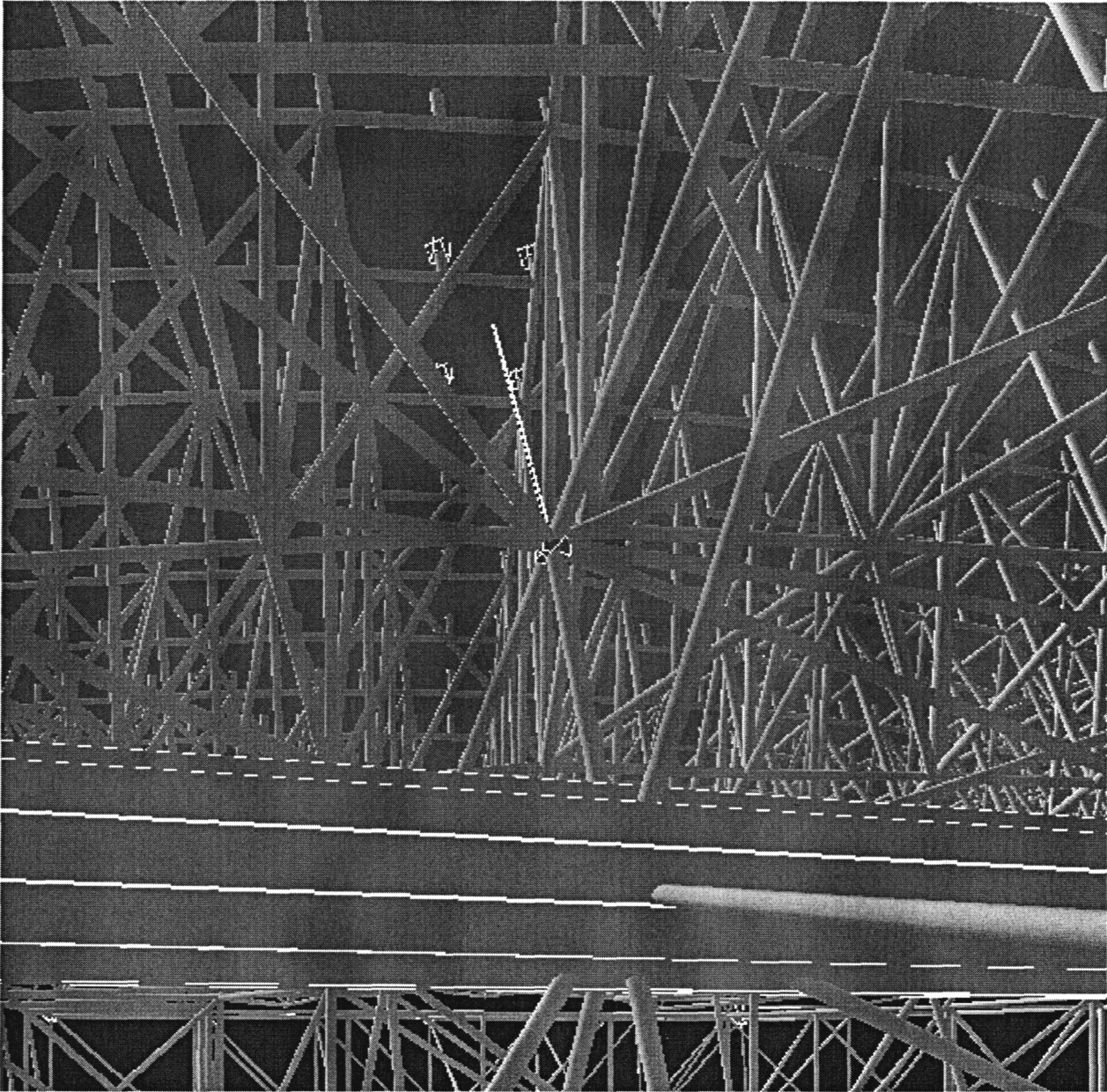Figure 17: A possible line-of-sight for the quadrant detector

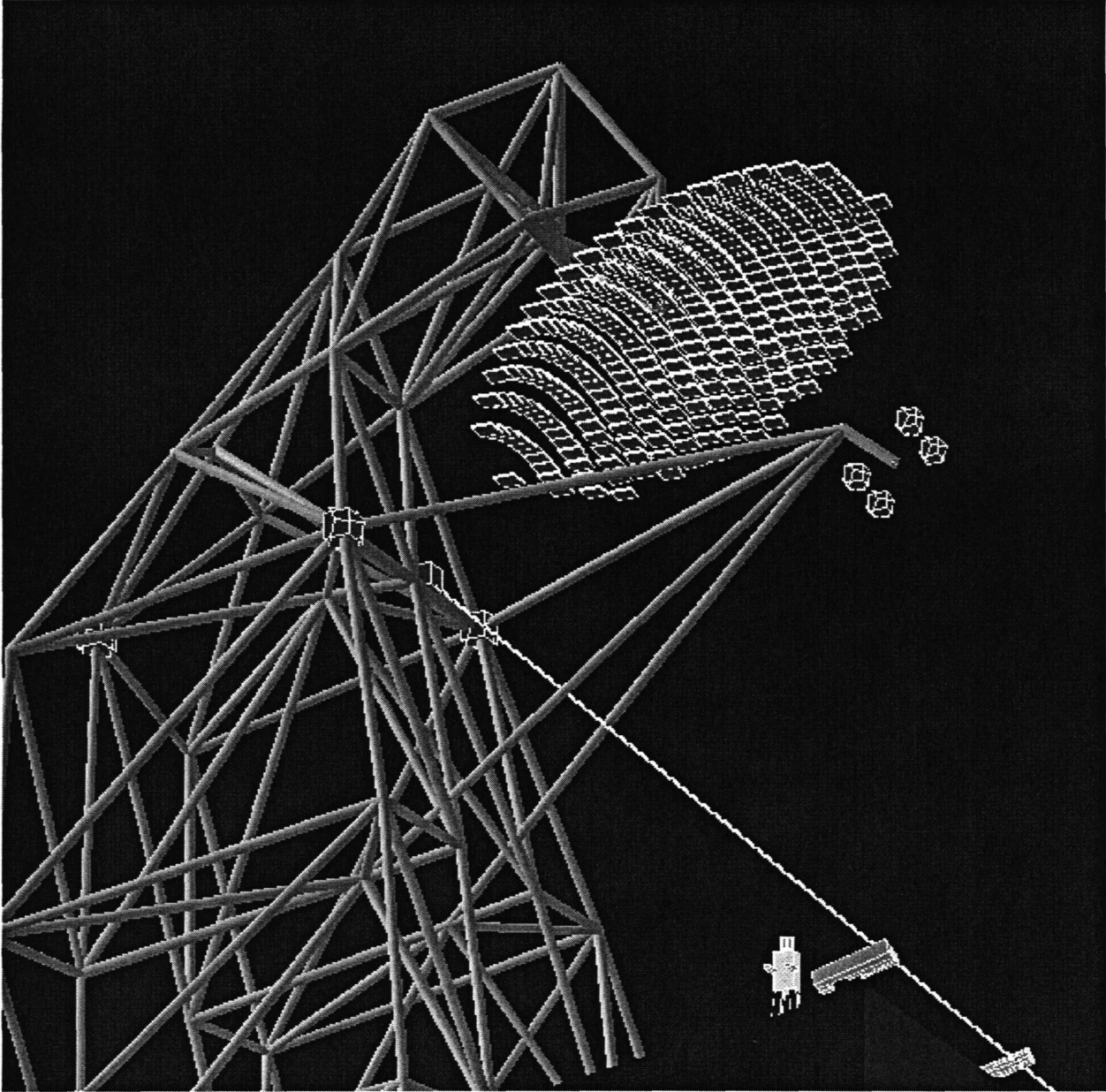Figure 18: The line-of-sight through from the transmitter at node 10230

Figure 19: The line-of-sight to the quadrant detector near the subreflector
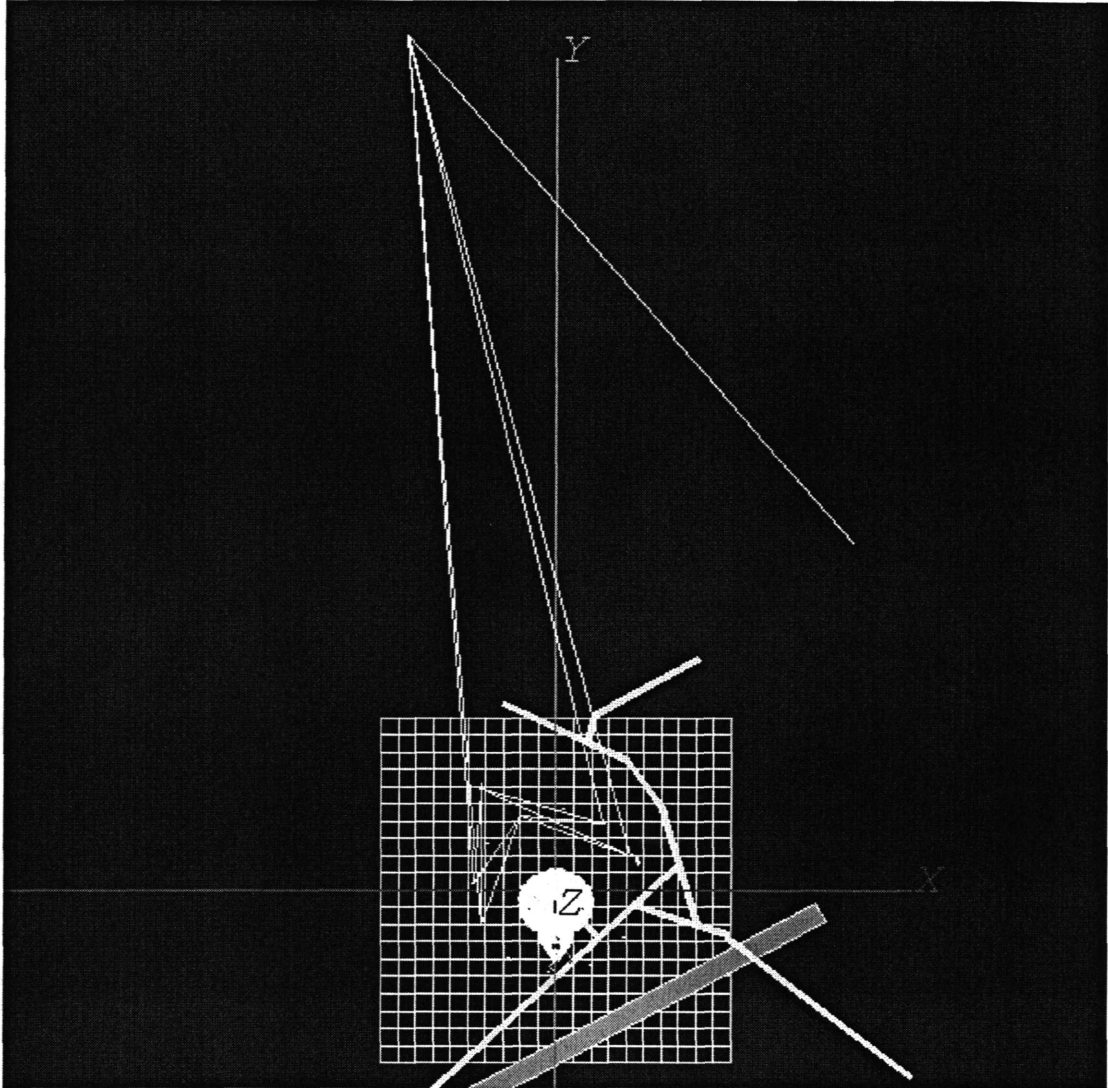
Figure 20: Looking down at lines-of-sight through the atmosphere

4   Atmospheric Measurements

The index of refraction of air varies by about a part per million per degree Centigrade. Wind and convection will result in patterns of temperature (index) variation moving through rangefinder lines-of-sight around the telescope, and will produce systematic and random errors of trilateration measurements. During the development of the rangefinder technology a variety of measurements have been made to study the effects of these errors, and such measurement campaigns are likely to continue. The purpose of the figures in this section is to illustrate how a number of rangefinders ranging on the same targets can sample multiple lines through the moving pattern of variations.

In Figure 20[33] four of the twelve groundbased rangefinders are ranging on reflectors on the weather tower and on a hillside about one kilometer north of the GBT. The path on the right side of the figure is from the "ZY10" rangefinder location being used for the 140-foot tests, ranging on the same hillside reflector. It is clear that if the wind is blowing approximately east-west there should be some degree of correlation of range

---

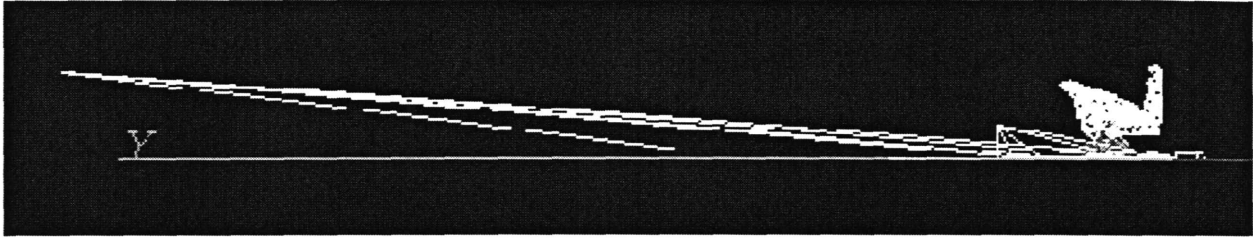[33]atlas980220i.ps [0,20000,80000]↦[0,20000,1800]43°[0,1,0]

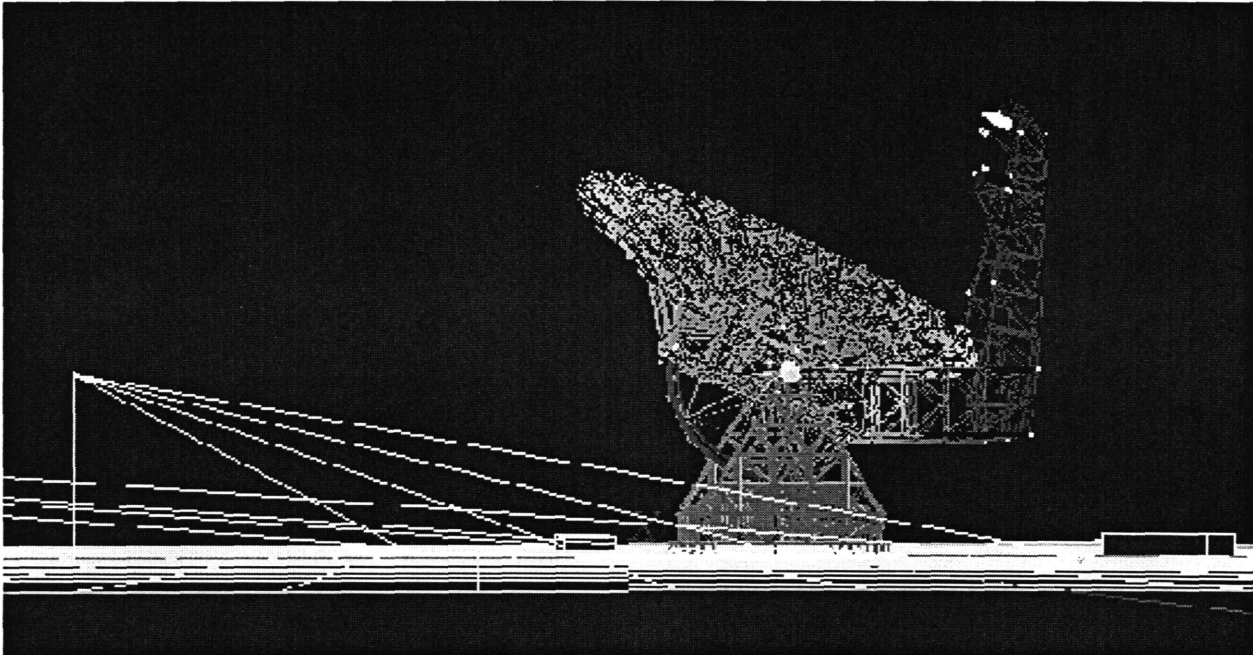Figure 21: Lines-of-sight through the atmosphere (looking east)

Figure 22: Lines-of-sight through the atmosphere (looking east)

residuals, but with a time lag of 10 to 30 s for a 6 m/s wind.

Figures 21[34] and 22[35] show the same lines from the side. The typical height of the lines above the ground is about 50 m. Measurements of the lines to the weather tower and to the GBT alidade (e.g., to the elevation bearings) should show correlated residuals if the wind is from the northwest or the southeast. Although such data can never completely sample the moving atmosphere, it is likely that they will yield valuable insights into the statistical properties of the atmosphere which affects our trilateration measurements.

Anyone who is interested in experimental designs for the sort of atmospheric measurements discussed above should read Holdaway and Radford's recent discussion [HR98] of possible experimental designs for somewhat analogous measurements associated with the MMA project. Their report contains a number of thought-provoking figures!

---

[34] atlas980220j_crop.ps [-80000,23000,0]↦[0,23000,1900]43°[0,0,1]
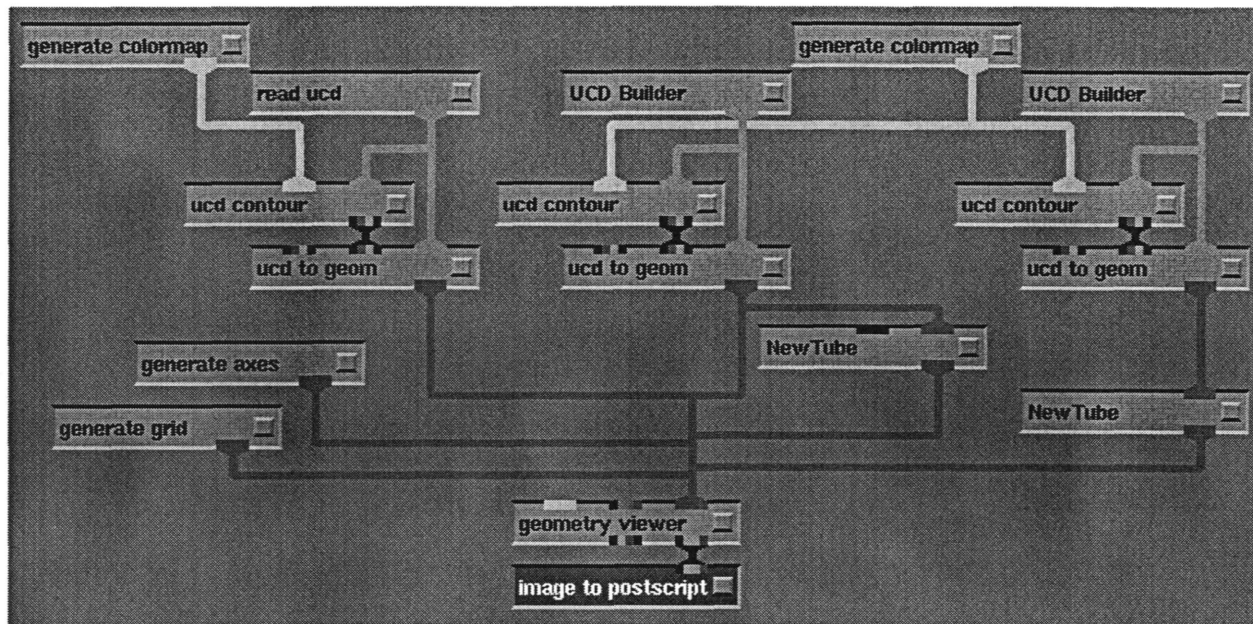[35] atlas980211c_crop.ps [-20000,3000,360]↦[0,1500,1900]35°[0,0,1]

Figure 23: The AVS network

5 About the AVS visualization system

Figure 23 shows the AVS network programming interface. The named boxes represent modules (programs), and they are connected by pipes, with the color codes of the pipes indicating the different types of data being passed from module to module. In the network shown in Figure 23, two different NASTRAN structural models (the alidade structure and the tipping structure) are being read by the two executions of the "UCD Builder" module, which converts NASTRAN output files to AVS "unstructured-cell-data" [UCD]. The module "read ucd" reads a data file which describes the set of rectangular solids in various sizes and orientations which represent the laser rangefinders, cardinal points, buildings, roads, human stick figures, etc., which we are displaying with the finite-element structural models. Several generator modules add the axes and the coordinate grid which represents the ground. The outputs of these pipelines are combined as input to the "geometry viewer", which renders the imagery. AVS has a graphical editor tool with which the network can be modified interactively; this is the toolkit-plus-visual-programming paradigm which is also used in several other scientific visualization systems (e.g., Khoros[36] and IBM's Data Explorer[37]).

The reader should be aware that we are *not* attempting to do "virtual reality" with the AVS system! The information content of the NASTRAN models as translated by the UCD Builder is merely lines connecting points – in order to create an illusion of finite size we use the "New Tube" module to create a cylinder around each line. We can specify the radius of each cylinder. However, this means that we have only two sizes of cylinders in these scenes, the alidade size (24 inches) and the tipping structure size (8 inches); the real GBT has many more different sizes, and many of its members have rectangular, not cylindrical, cross-section. This deficiency does not prevent geometric analysis, it merely means that the images must be interpreted carefully in critical cases, and that in any situation where beam sizes or cross-sections matter we must adjust the cylinder diameters to an appropriate value for the beams in question. Many details of the real GBT structure simply do not appear in these models: in order to calculate the structural deflections it was sufficient to lump together the masses of the details near a node and put the combined mass at the node point. The *pseudocolors* (not real colors) used in the renderings generally represent the magnitudes of the structural deflections due to gravity. For example, in Figure 10 (p.14) the variations of grey level across

---

[36]http://www.khoros.unm.edu/

[37]http://www.almaden.ibm.com/dx/DXHome.html

the dish represent the slight departures of the shape of the dish from a perfect homologous paraboloid. Note that the details of the joints where beams come together are not represented in any way in these images, and that the stairs and elevator are not attached to the east half of the feedarm (although their masses were lumped into nearby nodes of the structural model).

The author will be able to operate the Charlottesville AVS system on ringtail to produce new scenes on request.[38] The setup time is about 15 minutes if ringtail is not in use. The setup of AVS is only partially automated: it involves a considerable number of interactive operations. The "from" and "to" camera coordinates are entered into a form by hand, *not* by mouse operations. The saving and printing of Postscript files is done manually. The learning curve for all of these (interactive) operations is formidable. In principle the AVS installation is portable to other computer systems, but licensing fees are a barrier in the current budget climate. In general, the practical approach for producing new scenes will be to plan a visit to the Charlottesville computer lab for a session of one to two hours with the author operating the system.

In principle, we should be able to display the structural model rotated to arbitrary Az/El; in 1994 we did produce a set of such images.[39] However, in practice it is tedious and technically difficult to coax the system into this state; also, recent attempts have demonstrated that it does not work properly in the current version of the software.

In principle, we could render stereo pairs of images with AVS. The author expects that this would make only a modest improvement in our ability to perceive the geometry of the structure.

Future projects may need to use a different visualization system. It is likely that IBM's Data Exploder [DX] product could be substituted for AVS in this application. It is also likely that any new visualization hardware would be faster than the circa-1991 ringtail system, which needs about three seconds to re-compute these images, even with the aid of its graphics accelerator hardware.

The AWK program[40] which computes the input file for the "read ucd" module will be a useful starting point for any port of this application to DX, or for similar projects. This code draws rectangular solids in arbitrary orientation. "Cylinders" are drawn as six such solids, rotating through successive 30° steps to cover 180°, with the same rotation axis (see Figure 8, p.10). A "ball" is drawn as two coincident cubes, with the second cube rotated about X and Z such that some of its corners are in the faces of the first (see Figure 19, p.24). More complicated objects, such as rangefinders, are synthesized as combinations of rectangular solids, cylinders and balls (see Figure 14, p.17).

6 Acknowledgement

---

[38]The hardware and software maintenance contracts for ringtail and the other IBM RS/6000 systems at NRAO ended 1997-12-31, and were not renewed. The special display controller on ringtail failed during 1997 and was replaced by the controller from the other visualization workstation at the AOC in Socorro. Eventually some component will fail which cannot be replaced, and that will be the end of our AVS capability in Charlottesville. Potential users of this unique visualization capability should not wait, they should act *now*.

[39]See Figure 2 of http://www.cv.nrao.edu/ dwells/adass4c.ps, which gives an impression of the duty cycle of lines-of-sight through the box structure for $E = 45°$.

[40]/home/fits/dwells/avs_stuff/data/cube2.awk (44 KB)

References

[Gol97]   M. A. Goldman. Laser distance measurements to the elevation bearing support weldments. GBT Memo 164, National Radio Astronomy Observatory, March 1997. "..for any alidade azimuth, at least two ranging lines of sight are available on the right side of the alidade and two or more on the left side, to the bottom surface of each weldment.. the horizontal angle of the line between the [bearings] could be measured withing 1 arcsecond, and the vertical tilt of this line to 2 arcseconds.. ball retroreflectors.. would have to be viewed near the limits of their response range to return signal to both right and left side rangefinders..".

[HGPP98]   R. Hall, M. A. Goldman, D. H. Parker, and J. M. Payne. Measurement program for the Green Bank Telescope. In [TBD person], editor, *Astronomical Telescopes and Instrumentation*, volume [TBD] of *SPIE Proceedings*, page [TBD], Bellingham, WA, March 1998. Society of Photo-Optical Instrumentation Engineers. Paper 3357-29 of "Advanced Technology MMW, Radio and Terahertz Telescopes" conference held Kona, HI, 20-28 March 1998.

[HR98]   M. A. Holdaway and S. J. E. Radford. Options for placement of a second site test interferometer on Chajnantor. MMA Memo 196, NRAO, February 1998.

[Kin94]   Lee King. GBT coordinate systems. Limited-distribution memo, January 1994.

[Kin96a]   Lee King. Cardinal points on feedarm and box/wheel structures. Email to D.Parker, D.Hogg, D.Wells, F.Schwab, R.Lacasse, D.Seaman, S.Smith, R.Norrod and R.Hall, 4 April 1996. This memo lists the node-IDs or coordinates of 14 points on the secondary optics, 8 near the elevation bearings, 20 on the box/wheel and horizontal feedarm and 12 on the back of the reflector backup structure. These "cardinal points" are recommended locations for retroreflector prisms for monitoring structural deflections.

[Kin96b]   Lee King. Cardinal points on the reflector surface. Email to D. Parker, D. Hogg, J. Payne, D. Seaman, F. Schwab, D. Wells, R. Norrod and R. Hall, 22 February 1996. The file ftp://ftp.cv.nrao.edu/NRAO-staff/lking/mod95b.ps.feb2296 contains a map of a set of nodes whose deflections will determine the pointing of the main dish.

[KM93]   Lee King and Greg Morris. Foci arrangement and coordinate systems for the GBT. GBT Drawing C35102M081, NRAO, December 1993. The first sheet of this set of five drawings schematically defines six different coordinate systems to be used in the GBT project. Sheets 2-5 define the algebraic relationships between these coordinate systems.

[Nor96]   Roger D. Norrod. On possible locations for a GBT quadrant detector. GBT Memo 143, National Radio Astronomy Observatory, January 1996. Several nodes in the tipping structure are considered as locations for the quadrant detector transmitter. The structural model functions [WK95] are used to model the signal outputs.

[Par96]   David H. Parker. Round 2 of the rangefinder locations. Email to D.Wells, D.Seaman, G.Morris, J.Payne, R.Norrod, D.Hogg and R.Hall., 21 February 1996. This message specified the identification of rangefinder names ZY113 through ZY118 with specific coordinates on the feedarm.

[Pay95]   J. M. Payne. Monitoring the GBT arm movement. GBT Memo 144, National Radio Astronomy Observatory, December 1995. This memo discusses probable motions of the feedarm, and recommends development of the quadrant detector. It also recommends use of accelerometers and installation of retroreflectors at the ends of the elevation axle to be viewed through holes in the primary mirror.

[PS96]   J. M. Payne and D. Schiebel. First tests of a quadrant detector. GBT Memo 149, National Radio Astronomy Observatory, March 1996. "..laser transmitter was set up.. under the.. water tower..

detector.. 33.5 meters above the transmitter.. rms of each one minute.. range from 20 microns to 110 microns..".

[Sch96]   Frederic R. Schwab. Laser rangefinder locations and orientations. GBT Memo 147, National Radio Astronomy Observatory, March 1996.

[Wel94]   D. C. Wells. Visualization of GBT geometry. In R. A. Shaw, H. E. Payne, and J. J. E. Hayes, editors, *Astronomical Data Analysis Software and Systems IV*, number 77 in ASP Conference Series, pages 148–151, San Francisco, September 1994. ADASS, Astronomical Society of the Pacific. Poster paper at ADASS-IV meeting held at Baltimore, MD, 25-28 September 1994; see http://www.cv.nrao.edu/~dwells/adass4c.ps. Abstract: AVS [Advanced Visual Systems] has been used to explore lines of sight through the complex geometry of the Green Bank Telescope [GBT]. Perspective images computed by AVS from geometric descriptions of the components of the telescope have been used when selecting locations for the installation of laser rangefinders and when checking geometrical relationships along the optical path. The success of this application demonstrates the flexibility of the toolkit-plus-visual-programming paradigm for scientific visualization.

[WK95]   Don Wells and Lee King. The GBT Tipping-Structure Model in C. GBT Memo 124, NRAO, March 1995. Abstract: The finite element model of the GBT tipping structure has been translated into executable code expressed in the C language, so that it can be used by the control software modules for the pointing, focus-tracking, quadrant detector, active-surface and laser-rangefinder subsystems of the GBT. We give a description of this C-code version of the tipping structure model and two examples of its application to practical problems. See ftp://fits.cv.nrao.edu/pub/gbt_dwells_doc.tar.gz for the current revision of this memo (124.3 as of 1997-06-23).